Journal of Nuclear Materials 446 (2014) 240–245

Contents lists available at ScienceDirect

Journal of Nuclear Materials

journal homepage: www.elsevier.com/locate/jnucmat

Fracture behaviour of polycrystalline tungsten

Ermile Gaganidze *, Daniel Rupp, Jarir Aktaa

Karlsruhe Institute of Technology (KIT), Institute for Applied Materials, Hermann-von-Helmholtz-Platz 1, 76344 Eggenstein-Leopoldshafen, Germany

ARTICLE INFO

Article history:
Received 12 April 2013
Accepted 1 November 2013
Available online 10 November 2013

ABSTRACT

Fracture behaviour of round blank polycrystalline tungsten was studied by means of three point bending Fracture-Mechanical (FM) tests at temperatures between RT and 1000 °C and under high vacuum. To study the influence of the anisotropic microstructure on the fracture toughness (FT) and ductile-to-brittle transition (DBT) the specimens were extracted in three different, *i.e.* longitudinal, radial and circumferential orientations. The FM tests yielded distinctive fracture behaviour for each specimen orientation. The crack propagation was predominantly *intergranular* for longitudinal orientation up to 600 °C, whereas *transgranular cleavage* was observed at low test temperatures for radial and circumferentially oriented specimens. At intermediate test temperatures the change of the fracture mode took place for radial and circumferential orientations. Above 800 °C all three specimen types showed large ductile deformation without noticeable crack advancement. For longitudinal specimens the influence of the loading rate on the FT and DBT was studied in the loading rate range between 0.06 and 18 MPa $m^{1/2}$/s. Though an increase of the FT was observed for the lowest loading rate, no resolvable dependence of the DBT on the loading rate was found partly due to loss of FT validity. A Master Curve approach is proposed to describe FT vs. test temperature data on polycrystalline tungsten. Fracture safe design space was identified by analysis compiled FT data.

1. Introduction

The in-vessel components of a long term energy generation Demonstration fusion reactor (DEMO) will be exposed to high thermo-mechanical and neutron loads. The thermal load level of helium cooled divertor components of DEMO is estimated to at least 10 MW/m^2 [1]. Development and qualification of suitable high temperature structural materials belong to the key activities of the structural materials R&D within Tungsten and Tungsten Alloys (WWALLOY) program of the EFDA Topical Group on Fusion Materials [2]. Due to its numerous favourable properties, *e.g.* highest melting point among all metals (T_m = 3693 K), the lowest vapour pressure ($P_v = 1.3 \times 10^{-7}$ Pa at T_m), low sputter yield, high thermal conductivity, good thermal shock resistance, good high temperature strength and nearly zero tritium retention, tungsten belongs to the prominent candidate materials for application in divertor components [3]. The inherent low fracture toughness (FT), high ductile-to-brittle-transition temperature (DBTT) and low recrystallization temperature, however, belong to the limiting factors for the structural application of tungsten alloys and indicate further needs for material development.

Fracture-Mechanical (FM) properties of commercially available polycrystalline tungsten alloys have been extensively investigated in literature see *e.g.* [4–6]. The fracture behaviour was shown to strongly depend not only on the composition of the alloys but also on the material fabrication details and characteristic grain structure and texture within the grains. For technically pure tungsten (99.97% purity) no clear correlation was observed between the occurrence of *intergranular fracture* and grain boundary impurity content [7]. In the case of rolled polycrystalline tungsten rod studied in [5], the elongated grains parallel to the rolling direction (RD) together with the pronounced ⟨1 1 0⟩ fibre structure within the grains in the RD lead to pronounced anisotropic fracture behaviour. Namely the specimens extracted along the rolling direction exhibited twice as high fracture toughnesses and the significantly reduced DBTT than the other two investigated orientations. Moreover, the DBTT of polycrystalline tungsten was found to strongly depend on the deformation rate and to follow an Arrhenius relationship with an activation energy for the transition process between 1.05 and 1.44 eV [4,8] indicating the screw dislocations to control the ductile-to-brittle transition (DBT). The main objective of the current work is the investigation of the FM properties of the round blank polycrystalline tungsten in order to study the influence of the fabrication route specific anisotropic microstructure on the fracture behaviour and to enlarge the fracture toughness database on the novel tungsten alloys. Another objective of this work was the identification of the fracture safe design space on the base of current and the literature fracture toughness data on polycrystalline tungsten.

* Corresponding author. Tel.: +49 72160824083; fax: +49 72160824566.
E-mail address: ermile.gaganidze@kit.edu (E. Gaganidze).

0022-3115/$ - see front matter © 2013 Karlsruhe Institute of Technology (KIT). Published by Elsevier B.V. All rights reserved.
http://dx.doi.org/10.1016/j.jnucmat.2013.11.001

2. Experimental

Polycrystalline tungsten investigated in the current work was fabricated by Plansee Metall GmbH, Reutte/Austria through the powder metallurgic process. Some details of the fabrication route involving sintering into rods and subsequent forging into round blanks is given in [9]. Deformation degree achieved was ca. 80% and the final dimensions of the round blank were $\varnothing = 180$ mm and *height* = 30 mm [9]. In the current work the FM properties were studied by means of *quasi-static* three point bending (3 PB) experiments in a temperature range from room temperature (RT) to 1000 °C and under high vacuum condition. Miniaturized bend specimens of KLST geometry with outer dimensions of $27 \times 4 \times 3$ mm^3 and with a 1 mm deep U type notches were used for fracture toughness investigation. A nominal notch radius after electrical discharge machining (EDM) was 0.15 mm. To enhance stress triaxiality at the notch tip the EDM machined notches were further refined by application of a razor blade polishing [10]. Notch qualities were examined and overall notch lengths were measured under optical microscope. For the measurement of the notch size notch profiles on the both sides of the specimens were approximated by circles. The average circle radii were estimated for the majority of the specimens. The analysis of the radii distribution among 20 specimens yielded a mean radius of 25.6 μm and the standard deviation of 5.6 μm. The comparison of the RT facture toughness values for different pre-crack types in [10] showed that the results obtained by razor blade polishing technique were if at all only slightly above the values obtained on the specimens with sharp pre-cracks. The initial crack lengths varied in the range of 1040–1200 μm. The FM experiments were performed with a universal electro-mechanical testing machine from INSTORN equipped with a high temperature vacuum furnace allowing experiments in a temperature range between RT and 1600 °C. The *quasi-static* 3 PB tests were performed in a deformation controlled way at a deformation rates between 0.2 and 20.0 μm/s which corresponds to a stress intensity factor rate ($\dot{K}$) of 0.06–18 MPa m$^{1/2}$/s. The fracture surface morphology of the specimens was investigated by a scanning electron microscopy (SEM).

The microstructure of round blank tungsten is characterized by existence of platelet shaped grains being stacked parallel to a round blank base, see Fig. 1. To study the influence of the anisotropic microstructure on the FT and the ductile-to-brittle transition the specimens have been extracted in three different, *i.e.* longitudinal (L–R), radial (R–L) and circumferential (C–R) orientations, see Fig. 1c, where according to ASTM E399 the first letter denotes the specimen extraction direction and the second letter the expected direction of the crack propagation.

3. Results

Selected load vs. displacement curves of polycrystalline round blank tungsten for three different specimen orientations at an intermediate loading rate of 0.6–0.8 MPa m$^{1/2}$/s are shown in Fig. 2. All specimens failed by a brittle manner at RT without a noticeable plastic deformation. The load levels prior to fracture were considerably higher in R–L and C–R orientations than in L–R orientation. At intermediate temperatures the load levels prior to an unstable crack propagation increased for all three specimen orientations and the load vs. displacement curves for R–L and C–R orientations were characterized by crack emission and arrest events. For longitudinal orientation the lowest test temperature with an observable onset of plastic deformation in a load displacement curve was 400 °C whereas for the case of radially and circumferentially oriented specimens the deviations from linear load vs. displacement behaviour were observable at already 200 and 300 °C, respectively. Finally, at and above 800 °C a strong ductile deformation of the specimens without noticeable crack growth was observed for all three specimen orientations.

The SEM examination of the fracture surfaces revealed distinctive fracture behaviour for each investigated specimen orientation, see Fig. 3. At RT the specimen extracted in L–R orientation (Fig. 3a) failed by an *intergranular fracture*, while the specimens of R–L (Fig. 3b) and C–R (Fig. 3c) orientations exhibited a *transgranular cleavage*. With increasing the test temperature up to 600 °C crack propagation remained predominantly *intergranular* for L–R specimens as shown in Fig. 3d. For- R–L orientation the fracture behaviour changed from predominantly *transgranular* at RT (Fig. 3b) to predominantly *intergranular* (Fig. 3e) at intermediate temperatures. Still different fracture behaviour was observed for circumferentially oriented (C–R) specimens at intermediate temperatures which was characterized by a mixture of *transgranular cleavage* and *intergranular fracture* occurring in mutually orthogonal planes, see Fig. 3f.

In order to get more insight into crack initiation and propagation with increasing applied load, an *in situ* 3 PB test was conducted on R–L oriented specimen at 400 °C. The images near the notch tip were taken continuously while loading the specimen. The snapshots, at different deformation levels together with a corresponding load vs. displacement curve are shown in Fig. 4. Under increasing the applied load a deflection of the crack from the initial crack plane to a plane orthogonal to the initial crack plane is responsible for a change of fracture behaviour from *transgranular cleavage* to *intergranular fracture* observed under SEM in Fig. 3e.

The FT values obtained through the analysis of load vs. displacement curves in accordance to ASTM E399 are summarized in Fig. 5. The anisotropic microstructure is shown to have a strong influence on the FT and on the DBT. For the longitudinal orientation the material exhibits a low room temperature FT of about 7 MPa m$^{1/2}$ and a steep increase of FT above 200 °C. On increasing temperature the stress intensity factor loses its validity with increasing ductile behaviour and the calculated values give only a lower bound of FT. The corresponding invalid FT values are represented by open symbols in Fig. 5. In R–L and C–R orientations the material exhibits a relatively large room temperature FT of about 15 MPa m$^{1/2}$ and less steeper increase of FT with increasing temperature.

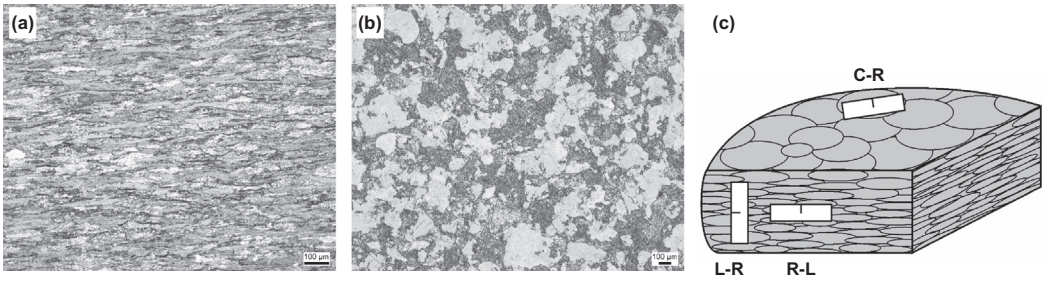

Fig. 1. Microstructure of polycrystalline round blank tungsten (a) plane transverse to base; (b) plane parallel to base; and (c) specimen orientations for the study of the influence of anisotropy on the fracture toughness.

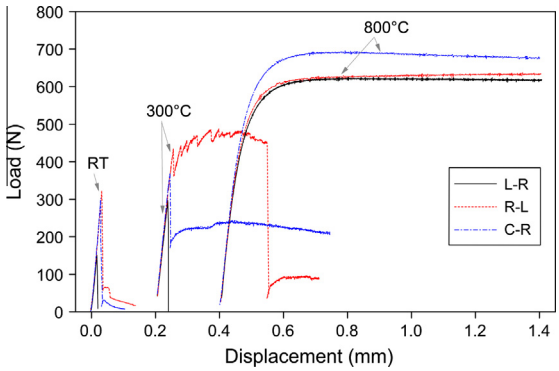

Fig. 2. Load vs. displacement for three different specimen orientations. Displacement controlled tests were performed at a loading rate of 2 μm/s corresponding to a stress intensity factor rate of 0.6–0.8 MPa $m^{1/2}$/s. The test temperature is indicated in the diagram. For a better visualization selected curves are shifted in abscissa.

L–R orientation was chosen for the investigation of the influence of the loading rate on the FT and DBT. The stress intensity factor rate ($\dot{K}$) was varied over *two* orders of magnitude between 0.06 and 18 MPa $m^{1/2}$/s. The load vs. displacement curves did not show any qualitative differences between different loading rates, though slightly improved ductility properties were observed for the lowest loading rate. The SEM investigation revealed a predominantly *intergranular fracture* at low and intermediate temperatures in the entire loading range. The calculated FT results are shown in Fig. 6. Though a noticeable increase of the FT is seen for the lowest loading rate at low temperatures, no resolvable dependence of DBT on the loading rate can be identified.

4. Discussion of results

The FM experiments yielded distinctive fracture behaviour for each investigated specimen orientation. For longitudinal orientation the material shows a low room temperature FT of about 7 MPa $m^{1/2}$, whereas for radial and circumferential orientations a

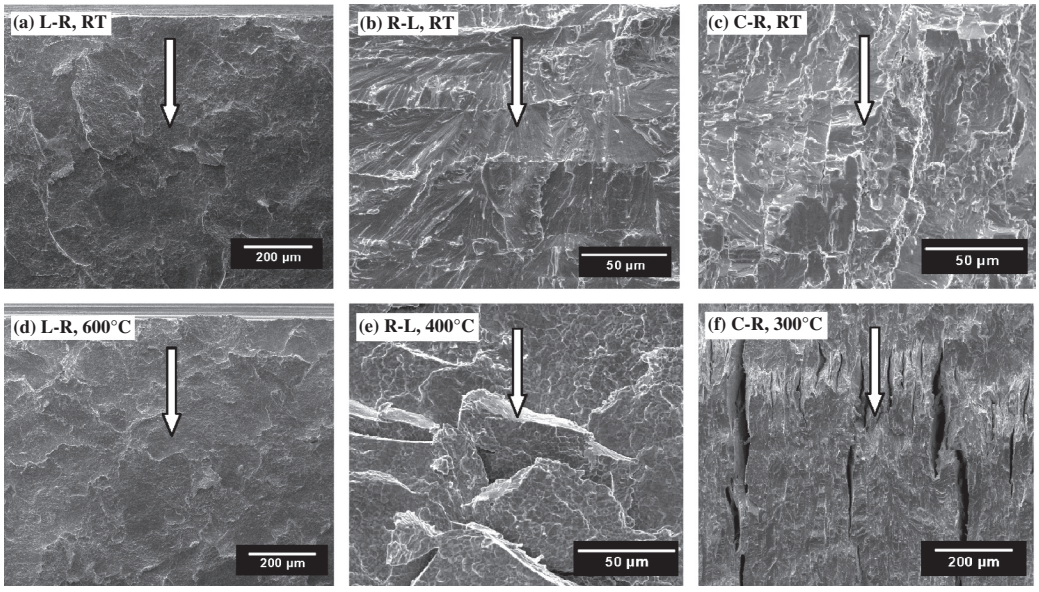

Fig. 3. SEM micrographs of fracture surfaces of polycrystalline round blank tungsten specimens tested at different temperatures. $\dot{K} = 0.6 - 0.8$ MPa $m^{1/2}$/s.

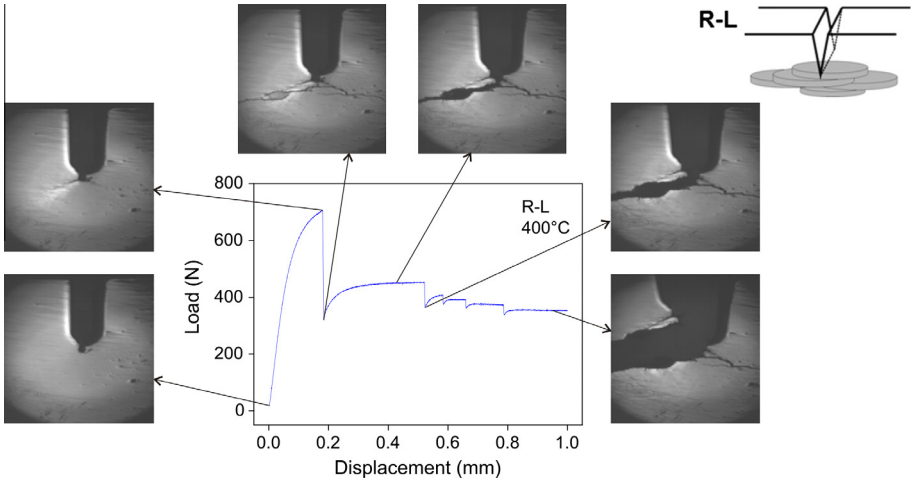

Fig. 4. In situ three point bend test conducted on R-L oriented specimen at 400 °C. The snap shots near the crack notch at different deformation levels. The sketch shows schematically the orientation of grains with respect to initial crack plane.

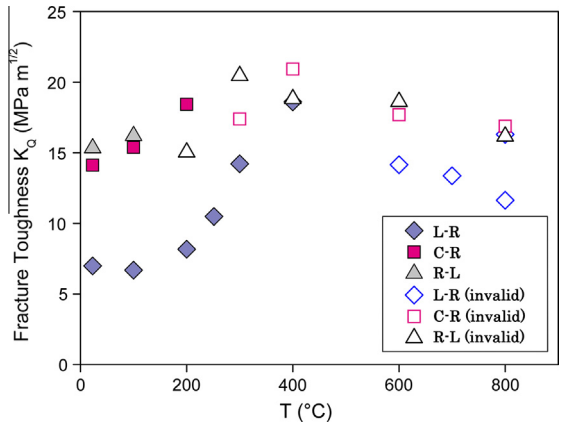

Fig. 5. Fracture toughness of round blank polycrystalline tungsten vs. test temperature for three different specimen orientations. Values denoted by open symbols do not satisfy the ASTM 399 validity criteria. $\dot{K}$=0.6–0.8 MPa m$^{1/2}$/s.

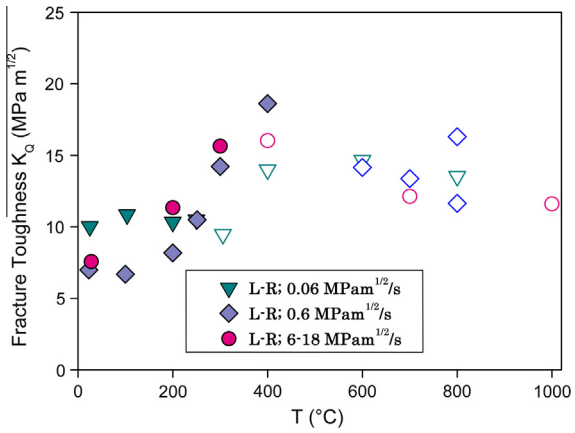

Fig. 6. Fracture toughness of round blank polycrystalline tungsten vs. test temperature for three different stress intensity factor rate levels. Values denoted by open symbols do not satisfy the ASTM 399 validity criteria.

relatively good FT of about 15 MPa m$^{1/2}$ is observed. Such behaviour can be qualitatively understood by considering the fabrication route specific anisotropic microstructure of polycrystalline round blank tungsten characterized by existence of platelet shaped grains being stacked parallel to a round blank base. In contrast to longitudinal orientation where under 3 PB the crack can be easily advanced by an *intergranular fracture*, for radial and circumferential orientations the crack is forced to propagate in a *transgranular* manner, see Fig. 3, which leads to an increase of apparent FT. Comparatively, for the case of rolled polycrystalline tungsten rod studied in [5] only the specimens extracted in the longitudinal orientation (with a crack plane transverse to the RD) showed a room temperature FT of about 15 MPa m$^{1/2}$, while the two other specimen orientations (with crack planes parallel to the RD) showed a low room temperature FT of about 7–8 MPa m$^{1/2}$. Fracture mechanical behaviour of round blank polycrystalline tungsten with good FT values in two of three investigated orientations is thus superior to fracture mechanical behaviour of commercially available rolled polycrystalline tungsten rods investigated *e.g.* in [5,8]. This observation indicates that it is the fabrication route specific microstructure that determines the anisotropic fracture behaviour of polycrystalline tungsten alloys. By considering the onset on nonlinear behaviour in load vs. displacement curves the DBTT can be estimated to be near 400 °C for longitudinal orientation which is in a reasonable agreement with the temperature evolution of the fracture toughness in Fig. 5. The DBTT is remarkably lower for radial and circumferential orientations as the deviation from linear load vs. displacement relationship is observed at temperatures between 200 and 300 °C. It has to be taken into account that in the two considered orientations the observed inelastic deformations in load vs. displacement curves must be related not only to the onset of ductile behaviour but also to the onset of complex fracture behaviour. So, on increasing the temperature the radially oriented specimens exhibits a deflection of the crack from the original crack plane and accompanied change of the fracture behaviour from a predominantly *transgranular cleavage* to a predominantly *intergranular fracture*. Such behaviour can be related to the increase of the resistance to *transgranular cleavage* with the temperature. As was shown in [5] with increasing the test temperature the transition from *transgranular cleavage* into *intergranular fracture* is expected when the fracture energy for the *intergranular fracture* becomes about one fourth of the fracture energy for the *transgranular cleavage*. In terms of the fracture toughness, the above mentioned transition is expected when the $K_{R-L} \geqslant 2K_{L-R}$ which is in a reasonable qualitative agreement with the current experiment.

The loading rate did not show an observable effect on the DBT. This can be partly related to a loss of fracture toughness validity in the transition range especially for the lowest loading rate. It has to be noted that though in the case of polycrystalline tungsten rod a strong loading rate dependence of DBTT was reported in [8] for *two* specimen orientations with the crack planes parallel to the RD, no clear trend was observable for the specimen orientation with an initial crack plane transverse to the RD. Moreover, taking into account an expected Arrhenius relationship between loading rate and the transition temperature, see *e.g.* [8], for a given ratio of the loading rate the lower is the absolute value of the DBTT the lower will be an expected shift in the DBTT. This circumstance is expected to make the observation of a possible dependence of the DBTT on loading rate for round blank polycrystalline tungsten with a relatively low DBTT difficult.

5. Brittle fracture safe design space

Aiming at the determination of the design space for a brittle fracture safe operation of components made out of tungsten we performed compilation of the fracture toughness data on polycrystalline tungsten including the results on disk and rod shaped materials, see Fig. 7. The data on polycrystalline rod material are from [10] and were also discussed in [5,8]. For a conservative assessment of the design space only fracture toughness data satisfying the ASTM 399 validity criteria and obtained in the weak orientations for given product forms have been implied. The weak orientations reflecting the material intrinsic fracture toughness are L-R orientation for the case of disk and C–R and R–L orientations for the case of rod shaped materials.

The Weibull model provides the probabilistic description of fracture behaviour relying on the weakest-link theory according to which failure of the weakest-link already results the failure of the whole system. The failure of the component takes place as soon as the local tensile stress in the vicinity of the weakest flaw (*i.e.* ahead of the crack tip) exceeds the characteristic critical stress of the material. Within the Weibull model the distribution of the fracture strength is due to the presence of the randomly distributed small flaws (cracks, second phase brittle particles, weak grain boundaries, etc.) in a component under consideration. The Weibull distribution can be applied equally well both to volume and surface flaws, see *e.g.* [11]. Generally speaking the Weibull distribution will depend on the component volume and application of the appropriate scaling laws are required for comparison of the

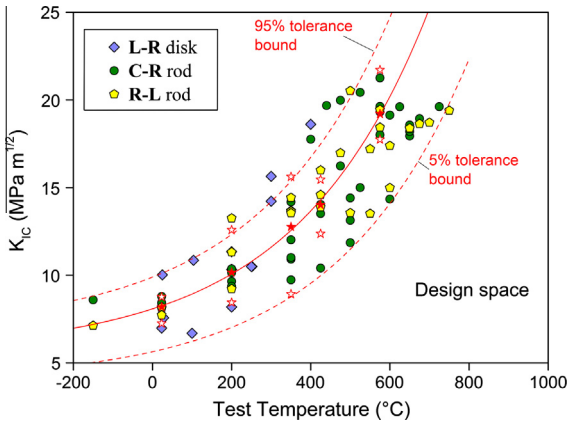

Fig. 7. Fracture toughness of polycrystalline tungsten vs. test temperature. The results on rod material stem from [10]. The full stars show calculated median fracture toughness corresponding to 50% cumulative failure probabilities, see text. The open stars show calculated fracture toughness corresponding 95% and 5% failure probabilities. The solid line is the least square fit to median fracture toughness with Master Curve type function given by Eq. (3). The dashed lines represent 95% and 5% tolerance bounds for fracture toughness calculated with Eq. (4).

specimens of different dimensions [11]. A failure of the component always emanates from the regions under tensile loading. The presence of the notch results the enhancement of the stress level ahead of the notch tip. For the determination of the fracture toughness (K_{IC}) in 3 PB tests on the notched specimens the modified stress distribution is accounted via using loading mode and specimen characteristic geometry factor [12]. The failure is still determined by the distribution of flaws in the stress field ahead of the notch tip. Thus the cumulative failure probability (P_f) of tungsten alloys can be assumed to follow the three parameter Weibull model, see *e.g.* [12,13].

$$P_f(T) = 1 - \exp\left\{-\left(\frac{K_{IC}(T) - K_{min}(T)}{K_o(T) - K_{min}(T)}\right)^{m(T)}\right\}, \quad (1)$$

where $K_o(T)$ is the fracture toughness corresponding to 63.2% cumulative failure probability, $K_{min}(T)$ is the lower bound fracture toughness and $m(T)$ is the Weibull exponent.

At a given temperature the estimates of cumulative failure probabilities were obtained with the following rank probability approximation [12]:

$$P_{rank} = \frac{i - 0.3}{n + 0.4}, \quad (2)$$

where i is the rank number and n is the number of points.

The Weibull model parameters K_o(T), $K_{min}(T)$ and $m(T)$ have been assessed for weak specimen orientations at five selected temperatures of 23, 200, 350, 425 and 575 °C by using Eqs. (1) and (2). Having obtained Weibull model parameters the fracture toughness values corresponding to 5%, 50% and 95% cumulative failure probabilities were calculated according to Eq. (1) and included in Fig. 7. The obtained model parameters describe probabilistic behaviour of intergranular fracture of the tungsten alloys in the weak specimen orientations and can be thus linked to the distribution of weak grain boundaries. The Weibull model analysis for the strong specimen orientations was not performed due to lack of the statistics in corresponding orientations and should be the subject of future investigations to find out a possible orientation dependence of Weibull exponent due to change of the fracture mode at low temperatures.

In analogy with the Master Curve (MC) approach, see ASTM E1925-05 [12], describing the behaviour of fracture toughness of ferritic steels in the transition range, the dependence of the calculated median fracture toughness values (corresponding to 50% failure probability) on test temperature was described by the following equation:

$$K_{IC} = A + B \cdot exp(C * (T - T_o)). \quad (3)$$

Within the MC approach the parameters A, B and C are fixed providing the best description of the common shape of fracture toughness vs. temperature curve for ferritic steels in the transition region and T_o is the reference temperature at which the median fracture toughness of ferritic steel specimens of a reference thickness equals to 100 MPa $m^{1/2}$. Due to absence of ASTM procedure for determination of the reference temperature T_o for tungsten alloys we applied a least square fitting to the median fracture toughness data in Fig. 7 with Eq. (3) with A, B, C and T_o as the fitting parameters. The best fit to the median fracture toughness was obtained with A = 5.63 MPa $m^{1/2}$, B = 8.93 MPa $m^{1/2}$, C = 0.00297 1/°C and T_o = 435.48 °C and is shown by a solid line in Fig. 7.

In Fig. 7 the fracture toughness values corresponding to 95% and 5% cumulative failure probabilities (open stars) give the statistical interval within which the fracture toughness data implied in the Weibull distribution analysis fall with the specified confidence. These values, however, cannot be used for the determination of the tolerance interval for the whole fracture toughness data set shown in Fig. 7 as a significant number of data point fall out of the interval. That is why and in analogy with the Master Curve (MC) approach [13] we calculated the tolerance bounds by applying the following equation:

$$K_{IC(0.xx)} = K_{min} + \left[\frac{In\left(\frac{1}{1-0.xx}\right)}{In(2)}\right]^{1/m(T)} \{A + Bexp[C(T - T_o)]\}, \quad (4)$$

where xx represents selected cumulative probability level, K_{min} is the lowest fracture toughness below which no cleavage fracture is expected at any temperature, A, B, C and T_o are parameters determined by fitting to median fracture toughness with Eq. (3), and m is the temperature dependent Weibull exponent. As the exponent m is known at selected temperatures only, we have used its average value of m_{av} = 7.24. K_{min} was omitted in Eq. (4) taking into account quite brittle behaviour of tungsten alloys at low temperatures. The calculated upper and lower tolerance bounds corresponding to 95% (xx = 0.95) and 5% (xx = 0.05) cumulative failure probabilities are shown in Fig. 7 by the dashed lines. The two lines confine the fracture toughness data set to a large extent. The area right to the lower tolerance bound is identified as brittle fracture safe design space for polycrystalline tungsten. For more conservative definition of the fracture safe design space the use of an even lower cumulative probability level (xx < 0.05) can be also considered. State of the art polycrystalline tungsten alloys fail by ductile tearing above 800 °C so that the shape of design space shown in Fig. 7 will be changed above 800 °C and expand to much higher stress intensity factors. The fracture safe design space analysis for tungsten alloys performed within the current work is the first attempt of this kind up to authors' knowledge and will require further validation for alternative fracture toughness dataset on tungsten alloys.

6. Summary

Fracture behaviour of round blank polycrystalline tungsten was investigated in a temperature range from RT to 1000 °C. *Quasi-static* three point bending experiments were performed on three different, *i.e.* longitudinal (L–R), radial (R–L) and circumferential (C–R), specimen orientations in order to study the influence of the fabrication route specific anisotropic microstructure on the fracture toughness and ductile-to-brittle transition. The material showed distinctive fracture behaviour for each investigated specimen

orientation. Longitudinal specimens failed by predominantly *intergranular fracture* up to 600 °C. The specimens extracted in radial and circumferential orientations, in contrast, failed by a *transcrystalline cleavage* at room temperature and exhibited complex fracture behaviour at elevated temperatures. Fracture toughness values were substantially larger for radial and circumferential specimen orientations in comparison to the longitudinal orientation up to 400 °C. At temperatures above 800 °C all three specimen types exhibited a large ductile deformation without a noticeable crack advance. The loading rate did not show an observable effect on the DBT for longitudinal orientation, though an increase of the fracture toughness was observed for the lowest load level. Superior fracture behaviour of polycrystalline round blank tungsten with two good fracture toughness orientations in comparison with rolled polycrystalline tungsten rod should give more flexibility for component designing. In combination with suitable shaping techniques, *e.g.* deep drawing, round blank tungsten may be very promising for fabrication of divertor finger module relevant components.

Compilation of fracture toughness data on polycrystalline tungsten has been performed for identification of the brittle fracture safe design space. Weibull analysis of the cumulative failure probability distributions were implied for calculation of fracture toughness values corresponding to specified confidence levels. Master Curve description is proposed for description of the temperature dependence of the median fracture toughness in the transition region. The upper and lower tolerance bounds constructed on the base of Master Curve were shown to fairly describe the scatter of the compiled fracture toughness data. The lower tolerance bound was used for identification of fracture safe design space.

Acknowledgements

This work, supported by the European Communities under the contract of Association between EURATOM and Karlsruhe Institute of Technology, was carried out within the framework of the European Fusion Development Agreement. The views and opinions expressed herein do not necessarily reflect those of the European Commission.

We thank Dr. Michael Rieth for providing the raw material.

References

[1] P. Norajitra, R. Giniyatulin, N. Holstein, T. Ihli, W. Krauss, R. Kruessmann, V. Kuznetsov, I. Mazul, I. Ovchinnikov, B. Zeep, Fus. Eng. Des. 75–79 (2005) 307–311.
[2] M. Rieth, S.L. Dudarev, S.M. Gonzalez de Vicente, J. Aktaa, T. Ahlgren, S. Antusch, et al., J. Nucl. Mater. 432 (2013) 482–500.
[3] N. Baluc, K. Abe, J.L. Boutard, V.M. Chernov, E. Diegele, S. Jitsukawa, et al., Nucl. Fusion 47 (2007) 696–717.
[4] A. Giannattasio, S.G. Roberts, Phil. Mag. 87 (2007) 2589–2598.
[5] D. Rupp, S.M. Weygand, Phil. Mag. 90 (2010) 4055–4069.
[6] B. Gludovatz, S. Wurster, A. Hoffmann, R. Pippan, Int. J. Refract. Met. Hard Mater. 28 (2010) 674–678.
[7] B. Gludovatz, S. Wurster, T. Weingärtner, A. Hoffmann, R. Pippan, Phil. Mag. 91 (2011) 3006–3020.
[8] D. Rupp, S.M. Weygand, J. Nucl. Mater. 417 (2011) 477–480.
[9] M. Rieth, D. Armstrong, B. Dafferner, S. Heger, A. Hoffmann, M.-D. Hoffmann, et al., Adv. Sci. Technol. 73 (2010) 11–21.
[10] D. Rupp, Bruch und Spröd-duktil-Übergang in polykristallinem Wolfram: Einfluss von Mikrostruktur und Lastrate, Karlsruhe Institute of Technology, Dissertation 2010: Shaker Verlag, 2010. Schriftreihe "Werkstoffwissenschaft und Werkstofftechnik", Band 61/2010.
[11] D. Munz, T. Fett, Mechanisches Verhalten keramischer Werkstoffe, Springer-Verlag, Berlin Heidelberg New York, 1989. ISBN 3-540-51508-9.
[12] K. Wallin, Eng. Fract. Mech. 69 (2002) 451–481.
[13] ASTM designation: E 1921-05, Standard test method for determination of reference temperature, T_o, for ferritic steels in the transition range. s.l., ASTM International, 100 Barr Harbor Drive, PO Box C700, West Conshohocken, PA 19428–2959, United States, 2005.